Handling Phase in Sparse Reconstruction for SAR: Imaging, Autofocusing, and Moving Targets

Müjdat Çetin, Özben Önhon
Faculty of Engineering and Natural Sciences, Sabancı University, İstanbul, Turkey

Sadegh Samadi
Department of Electrical and Electronics Engineering, Shiraz University of Technology, Shiraz, Iran

Abstract

We consider sparse image reconstruction methods for synthetic aperture radar (SAR) and discuss how issues related to the phase of the complex-valued SAR reflectivities and the phase of the observed SAR data emerge and are handled in a number of currently available methods. In particular, we consider analysis and synthesis models for sparsity-driven SAR imaging, and discuss how the optimization problems in both cases need to treat the magnitudes and the phases of the reflectivities separately. Then, we consider errors in the SAR observation model, due to, e.g., imperfect knowledge of the SAR sensing platform. Such errors lead to phase errors in the SAR data and cause defocusing of the formed imagery. We describe how joint imaging and phase error correction can be performed in a sparsity-driven imaging framework. Finally, we consider the problem of SAR imaging in the presence of moving targets in the scene, and describe how that leads to more complicated phase errors. We discuss how sparsity can be used to attack this problem as well. We present experimental results illustrating the behavior of the methods discussed.

1 Introduction

Sparsity has been of interest for synthetic aperture radar (SAR) imaging implicitly over many years, and more explicitly within the last decade [1]. Ideas based on sparse signal representation have recently led to advanced image formation methods offering a number of benefits for SAR, including increased resolvability of point scatterers, reduced speckle, and robustness to limitations in data quality and quantity [2, 3]. One aspect of SAR that differentiates it from incoherent imaging applications is that both the observed data and the reconstructed images involve complex-valued quantities. Hence signal processing methods need to deal with both the magnitude and the phase of the signals involved. In this paper, we emphasize this aspect of SAR imaging, and explore how issues related to phase emerge and are handled in sparse reconstruction methods for SAR.

We start with sparsity-driven SAR imaging via an analysis model. This model involves sparsity constraints on the reflectivity field and on the gradient of its magnitude. We describe how this leads to a more complicated sparse signal recovery problem than those arising in real-valued signal processing problems. We also consider a synthesis model for sparse representation in SAR imaging. This model leads to an optimization problem over the phase of the reflectivity field and the representation coefficients of its magnitude.

Then we consider the problem of model errors that result from, e.g., sensing platform position uncertainties, which lead to phase errors in the measured data, and consequently defocusing in the formed imagery. We describe a sparsity-driven method for joint imaging and autofocusing in the presence of such phase errors. This method estimates and corrects the phase errors in the process of image formation and exhibits the benefits of sparsity-driven imaging while performing autofocusing. Finally, we consider the problem of SAR imaging in the presence of moving targets in the scene, which also leads to phase errors. These errors cause spatially-varying defocusing in the scene. We discuss how the sparsity-driven autofocus framework mentioned above can be extended to treat this problem as well. We present limited experimental results illustrating the behavior of the methods discussed.

2 Phase in Image Reconstruction

In this section, we describe how the complex-valued nature of SAR reflectivities, and the resulting task of properly handling the magnitude and phase of the reflectivities has differentiated sparsity-driven SAR imaging from other imaging applications involving real-valued scene descriptions. In particular, we consider the analysis-based SAR imaging formulation of [2] (Section 2.1), and the synthesis-based formulation of [4] (Section 2.2). In an analysis model, sparsity is imposed on some transformation of the signal or image to be recovered, whereas in a synthesis model sparsity is imposed on the coefficients of an explicit dictionary used to represent the signal or image of interest. In both cases, the quantity that admits sparse representation in SAR is the reflectivity magnitude. We describe how this is treated in both formulations.

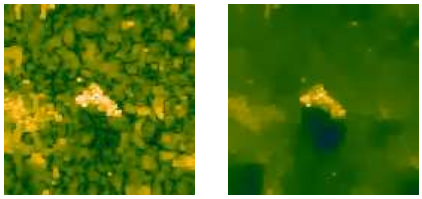

(a) (b)

Figure 1: Sparsity-driven SAR imaging using an analysis model imposing smoothness constraints. (a) Reconstructed field by smoothing real and imaginary components. (b) Reconstructed field by smoothing the magnitudes directly. (Taken from [5].)

2.1 Imaging via an analysis model

Let us start with the following linear observation model for SAR:

$$\mathbf{y} = \mathbf{H}\mathbf{f} + \mathbf{n}, \tag{1}$$

where $\mathbf{f}$ is the underlying, complex-valued reflectivity image, $\mathbf{H}$ is the mathematical model of the observation process, $\mathbf{y}$ denotes the measured phase history data, and $\mathbf{n}$ accounts for additive measurement noise. In [2], an estimate of $\mathbf{f}$ is obtained by minimizing the following cost function:

$$J(\mathbf{f}) = \|\mathbf{y} - \mathbf{H}\mathbf{f}\|_2^2 + \lambda_1 \|\mathbf{f}\|_p^p + \lambda_2 \|\boldsymbol{\nabla}|\mathbf{f}|\|_p^p. \tag{2}$$

Here $\|\cdot\|_p$ denotes the ℓ_p-norm, $\boldsymbol{\nabla}$ is a discrete approximation to the 2-D derivative operator (gradient), $|\mathbf{f}|$ denotes the vector of magnitudes of the complex-valued vector $\mathbf{f}$, and λ_1, λ_2 are scalar parameters. The values used for p are around 1, so the second and third terms enforce sparsity. The relative contribution of these two terms are determined through the choice of the hyperparameters λ_1 and λ_2. The second term indicates a preference for spatially sparse reflectivity fields. The third term enforces sparsity on the gradient of the reflectivity magnitudes, indicating a preference for piecewise smooth reflectivity magnitude fields. Such smoothness is expected within homogenenous natural terrain types in SAR, and within some man-made structures. Even in homogeneous regions, the phases of the reflectivities in spatially neighboring pixels however are generally uncorrelated, hence no such smoothness is expected in phase. As a consequence, we need to impose sparsity on $\boldsymbol{\nabla}|\mathbf{f}|$, and not on $\boldsymbol{\nabla}\mathbf{f}$, as the latter would lead to smoothing of the real and imaginary parts of the reflectivity field, which may not lead to the desired smoothing effect on the magnitudes. Having to use a penalty on the magnitudes makes the optimization problem in (2) more challenging than its counterparts in real-valued sparse signal recovery problems. This has been studied in [2], and later in [3], and an algorithm based on half-quadratic regularization has been proposed. In Figure 1, we show a SAR image reconstructed using this algorithm, together with an image that would be obtained if the smoothness penalty was directly on $\mathbf{f}$ (hence its real and imaginary parts). We observe that treating the magnitude and the phase separately leads to a result with suppressed speckle and preserved region boundaries.

2.2 Imaging via a synthesis model

In an analysis model, sparsity is imposed on some transformation of the signal of interest, as in the gradient-based penalty in the third term of (2). On the other hand, in a synthesis model, we represent the signal of interest in terms of a dictionary and impose sparsity on the dictionary coefficients. There is ongoing debate on similarities and differences between these two perspectives. We will just focus on one particular issue of interest for us. We note that (2) uses two different regularization terms one imposing the sparsity of the field, and the other its piecewise smoothness. These two terms are used together to handle cases in which one of these terms does not serve as a good enough constraint throughout the scene. However, (2) imposes these two potentially conflicting constraints jointly everywhere in the scene, leading to some degree of inconsistency with the stated objective. This issue may be handled in a more consistent manner within a synthesis model. In particular, one can form an overcomplete dictionary consisting of atoms corresponding to the different types of constraints in (2). As the atoms can also exhibit spatial locality, one or the other type of sparsity can be "active" at a particular location in the scene, avoiding simultaneous use of potentially conflicting constraints. Furthermore, this perspective can, in principle, allow the combined use of a variety of other signal dictionaries, leading to preservation of multiple feature types in a single scene. Based on these thoughts, a synthesis model for sparsity-driven SAR imaging has been proposed in [4]. As in (2), what admits sparse representation is the magnitude of the reflectivity field $\mathbf{f}$. Hence we are interested in a representation of the form $|\mathbf{f}| = \boldsymbol{\Psi}\boldsymbol{\alpha}$, where $\boldsymbol{\Psi}$ is an overcomplete dictionary with the coefficient vector $\boldsymbol{\alpha}$. Let us also write $\mathbf{f} = \boldsymbol{\Theta}|\mathbf{f}|$, where $\boldsymbol{\Theta}$ is a diagonal matrix, the i-th diagonal element of which is $e^{j\gamma_i}$, with γ_i indicating the unknown phase of the i-th scene element $\mathbf{f}_i$. Based on this notation, we can rewrite the observation model as:

$$\mathbf{y} = \mathbf{H}\mathbf{f} + \mathbf{n} = \mathbf{H}\boldsymbol{\Theta}\boldsymbol{\Psi}\boldsymbol{\alpha} + \mathbf{n}. \tag{3}$$

Letting $\boldsymbol{\theta}$ be a vector consisting of the diagonal elements of $\boldsymbol{\Theta}$, we can write the following cost function to be minimized for SAR imaging:

$$J(\boldsymbol{\alpha}, \boldsymbol{\theta}) = \|\mathbf{y} - \mathbf{H}\boldsymbol{\Theta}\boldsymbol{\Psi}\boldsymbol{\alpha}\|_2^2 + \lambda\|\boldsymbol{\alpha}\|_p^p \;\; s.t. \;\; |\boldsymbol{\theta}_i| = 1 \quad \forall i$$

We note that the variables to be optimized involve the phase of the field, and the representation coefficients for its magnitude. This problem can be solved using the coordinate descent algorithm developed in [4]. Figure 2 contains results on a synthetic scene demonstrating how this approach can be more effective than the analysis-based approach of Section 2.1 in scenes exhibiting multiple feature types.

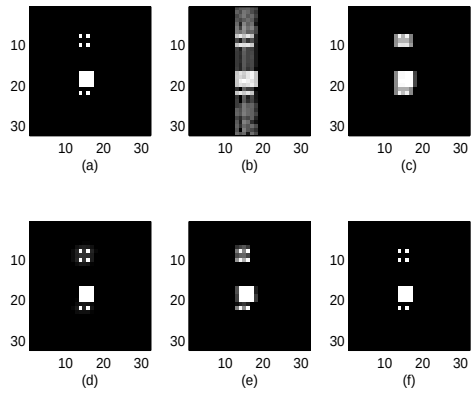

Figure 2: SAR imaging of a synthetic scene. (a) Synthetic scene. (b) Conventional polar-format reconstruction. (c) Result of the analysis-based formulation of Section 2.1. (d)-(f) Results of the synthesis-based formulation of Section 2.2 using various dictionaries: (d) A shape-based dictionary of spikes and squares, (e) Wavelet dictionary, (f) Spike-wavelet overcomplete dictionary. (Taken from [4].)

3 Phase Errors: Autofocusing and Moving Targets

In the previous section, we have seen examples of how the phase of the imaged scene is handled in sparsity-driven SAR imaging. Now we turn to the phase of the measured phase history data. Accurate measurement of the phase is of course critical for obtaining an accurate SAR image. However, various uncertainties, e.g., in the position of the SAR platform, lead to demodulation time errors, which in turn cause phase errors. Such phase errors result in defocusing of the reconstructed imagery. Because of the defocusing effect of such errors, the techniques developed for removing phase errors are often called autofocus techniques [6]. In Section 3.1, we describe a method for joint sparsity-driven imaging and phase error correction, hence autofocusing. SAR assumes that the scene is stationary within the data collection interval. Moving targets in the scene cause artifacts including defocusing around the spatial neighborhood of the target in the scene. Motion of a target in the scene can also be modeled as a phase error over the phase history data corresponding to a stationary scene [7]. In Section 3.2, we describe a method for sparsity-driven imaging of moving targets.

3.1 Demodulation time errors

Errors in the distance between the SAR sensor and the scene center (due to, e.g., SAR platform position uncertainties or atmospheric delays) cause demodulation time errors [6], which in turn lead to phase errors. Since uncertainties on, e.g., the position of the platform, are constant over a signal received at one aperture position, but are different at each aperture position, phase errors caused by such uncertainties vary only along the cross-range direction in the frequency domain. Such phase errors cause defocusing of the image in the cross-range direction. The observation model in the presence of such phase errors can be expressed as

$$\mathbf{y} = \mathbf{H}(\boldsymbol{\phi})\mathbf{f} + \mathbf{n}, \tag{4}$$

where $\boldsymbol{\phi}$ denotes the length M vector of phase errors, where M denotes the number of aperture positions for data collection. The sparsity-driven autofocus (SDA) method [8] minimizes the following cost function for joint imaging and phase error estimation:

$$J(\mathbf{f}, \boldsymbol{\phi}) = \|\mathbf{y} - \mathbf{H}(\boldsymbol{\phi})\mathbf{f}\|_2^2 + \lambda\|\mathbf{f}\|_1. \tag{5}$$

The optimization problem is solved by a coordinate descent-based algorithm. Steps of the algorithm involve the use of the SAR imaging method of [2], as well as closed-form updates for phase error estimation. In Figure 3, we show an example of how SDA is able to generate a focused image from phase-corrupted data. Experiments in [8] also demonstrate the role played by the sparsity constraint in the autofocusing achieved by SDA.

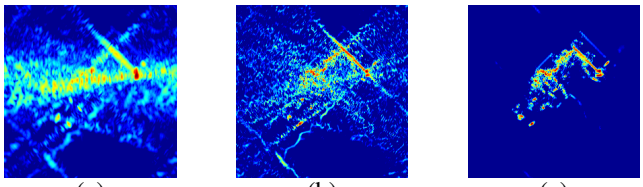

Figure 3: SAR imaging in the presence of phase errors. (a) Conventional imaging. (b) Sparsity-driven imaging without autofocusing. (c) SDA. (Taken from [8].)

3.2 Moving targets

We have mentioned that the effect of moving targets in the scene can also be viewed as phase errors. This is the same principle used in moving target indication (MTI). When we image a scene containing moving targets, we observe artifacts, including defocusing. However, unlike the scenario considered in Section 3.1, the defocusing in this case is not uniform throughout the scene, but rather is spatially-varying. In particular, we encounter no defocusing in the stationary parts of the scene, and the nature of the defocusing in the moving parts depends on the motion characteristics of the objects in that region. Hence, in contrast with the spatially-invariant focusing problem of Section 3.1, here we encounter a more complicated, spatially-variant focusing problem. As a result, we need to keep an account of the contributions from each spatial location to the phase error

at each aperture position. Let $\boldsymbol{\beta}_m$ be a vector capturing the phase errors for the m-th aperture position:

$$\boldsymbol{\beta}_m = \left[e^{j\phi_1(m)}, e^{j\phi_2(m)}, ..., e^{j\phi_I(m)}\right]^T. \quad (6)$$

Here $\phi_i(m)$ is the contribution of the i-th spatial location in the scene to the phase error at the m-th aperture position. We can then construct the length MI vector $\boldsymbol{\beta}$, which includes phase errors corresponding to all points in the scene, for all aperture positions: $\boldsymbol{\beta} = \left[\boldsymbol{\beta}_1^T, \boldsymbol{\beta}_2^T, ..., \boldsymbol{\beta}_M^T\right]^T$. Given this notation, [9] has proposed moving target SAR imaging by minimizing the following cost function with respect to the field and the phase errors:

$$J(\mathbf{f}, \boldsymbol{\beta}) = \|\mathbf{y} - \mathbf{H}(\boldsymbol{\phi})\mathbf{f}\|_2^2 + \lambda_1 \|\mathbf{f}\|_1 + \lambda_2 \|\boldsymbol{\beta} - \mathbf{1}\|_1 \quad s.t. \;\; |\boldsymbol{\beta}_i| = 1 \;\; \forall i \quad (7)$$

Here, $\mathbf{1}$ is a $MI \times 1$ vector of ones. Since the number of moving points is usually much less than the total number of points in the scene, most of the ϕ values in the vector $\boldsymbol{\beta}$ are zero. Since the elements of $\boldsymbol{\beta}$ are in the form of $e^{j\phi}$'s, when a particular element in ϕ is zero, the corresponding element in $\boldsymbol{\beta}$ becomes one. Therefore, this sparsity on the phase errors is incorporated into the problem by using the regularization term $\|\boldsymbol{\beta} - \mathbf{1}\|_1$. The formulation in (7) considers potential motion in all locations in the scene, however [9] also contains a modification through which one can focus on regions of interest in the scene that are more likely to contain moving objects. Figure 4 contains a synthetic example involving a scene containing several stationary point targets and two moving targets with constant velocities of $5m/s$ and $8m/s$ in the cross-range direction. Given the SAR system parameters used in this example, these two targets induce quadratic phase errors with a center to edge amplitude of 2.5π radians and 4π radians, respectively, over the synthetic aperture. In the results for conventional imaging and sparsity-driven imaging without any phase error correction, the defocusing and artifacts in the reconstructed images caused by the moving targets are observed. On the other hand, the image reconstructed by the sparsity-driven moving target imaging method is well focused.

4 Conclusion

We have discussed how issues related to the phase of the complex-valued SAR reflectivities and of the measured data emerge in sparse reconstruction problems for SAR, and how they are handled in a number of existing methods. With proper treatment of the complex-valued nature of SAR, sparse signal representation theory and methods offer valuable tools for SAR imaging of scenes that admit sparse representations.

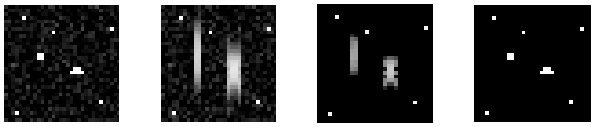

(a) (b) (c) (d)

Figure 4: Moving target SAR imaging. (a) Original scene. b) Image reconstructed by conventional imaging. c) Image reconstructed by sparsity-driven imaging assuming a stationary scene. d) Image reconstructed by the proposed moving target imaging method. (Taken from [9].)

5 Acknowledgments

This work was partially supported by the Scientific and Technological Research Council of Turkey under Grant 105E090, and by a Turkish Academy of Sciences Distinguished Young Scientist Award.

References

[1] L. C. Potter, E. Ertin, J. T. Parker, and M. Çetin, "Sparsity and compressed sensing in radar imaging," *Proc. of the IEEE*, vol. 98, pp. 1006–1020, 2010.

[2] M. Çetin and W.C. Karl, "Feature-enhanced synthetic aperture radar image formation based on nonquadratic regularization," *IEEE Trans. Image Processing*, vol. 10, no. 4, pp. 623–631, 2001.

[3] M. Çetin, W. C. Karl, and A. S. Willsky, "Feature-preserving regularization method for complex-valued inverse problems with application to coherent imaging," *Opt. Eng.*, vol. 45, no. 1. pp. 017003 1-11, 2006.

[4] S. Samadi, M. Çetin, and M. A. Masnadi-Shirazi, "Sparse representation-based synthetic aperture radar imaging," *IET Radar, Sonar and Navigation*, vol. 5, no. 2, pp. 182–193, 2011.

[5] M. Çetin, *Feature-Enhanced Synthetic Aperture Radar Imaging*, Ph.D. thesis, Boston Univ., 2001.

[6] C. V. Jakowatz, Jr., D. E. Wahl, P. H. Eichel, D. C. Ghiglia, and P. A. Thompson, *Spotlight-Mode Synthetic Aperture Radar: A Signal Processing Approach*, Springer, 1996.

[7] J. R. Fienup, "Detecting moving targets in SAR imagery by focusing," *IEEE Trans. Aerospace and Electronic Systems*, vol. 37, no. 3, pp. 794–809, 2001.

[8] N. Ö. Önhon and M. Çetin, "A sparsity-driven approach for joint SAR imaging and phase error correction," *IEEE Trans. Image Processing*, to appear.

[9] N. Ö. Önhon and M. Çetin, "SAR moving target imaging in a sparsity-driven framework," *SPIE Optics + Photonics Symposium, Wavelets and Sparsity XIV*, 2011.